

# MARINE ATMOSPHERIC BOUNDARY LAYER STRUCTURE ASSOCIATED WITH COASTAL LOW-LEVEL JETS

Akarshna K. Iyer

*Advisor: Ruben Delgado*

*Atmospheric and Planetary Sciences, Hampton University*

## **Abstract**

Atmospheric processes within the marine atmospheric boundary layer (MABL) strongly influence offshore wind structure and forecasting. This study examines coastal low-level jets (LLJs) and their relationship to temperature advection using observations and model output from the third Wind Forecast Improvement Project (WFIP-3). LLJs were identified from High-Resolution Rapid Refresh (HRRR) data, and a line integral method was implemented to quantify horizontal temperature advection during the events.

Southerly LLJs were hypothesized to correspond with warm air advection, but results reveal a more complex relationship. LLJ events cluster primarily in the southwest and northeast sectors, yet positive and negative temperature advection occur within both regions. A clearer structural distinction emerges with altitude changes as northerly LLJs tended to occur at higher levels, while southerly LLJs were detected more at lower levels. These observations suggest differing forcing mechanisms and motivate further investigation into the processes causing LLJ development and evolution.

Overall, these findings highlight the influence of synoptic and mesoscale processes on coastal LLJs and demonstrate that their thermodynamic structure is controlled by multiple factors. Improving the characterization of LLJ structure and associated temperature advection has direct implications for offshore wind forecasting and boundary layer representation, supporting Earth system science objectives within NASA.

## **Introduction**

### **Background**

The planetary boundary layer (PBL) is the layer of air closest to the Earth's surface. The marine atmospheric boundary layer (MABL) is a subset of the PBL; it is the layer above the ocean. The MABL is typically under two kilometers in depth, it is shallower than the PBL (over land) due to limited frictional influence over the water<sup>1</sup>.

The MABL's proximity to the surface allows it to encompass several important operations ranging from aviation and marine navigation to offshore energy generation and emergency response. It is incredibly important to understand the MABL and the processes occurring within it because they can affect these operations.

NASA has a recurring objective to explore Earth sciences and have expressed interest in the MABL through various missions and initiatives, specifically the advancement of remote sensing technologies and modeling capabilities<sup>2</sup>.

Wind speed and direction fluctuations within the MABL play a critical role in heat and moisture transport. Among the different wind phenomena that occur in the MABL, low-level jets are particularly important due to their concentrated regions of enhanced wind speed and associated dynamics.

### **Low-level Jets**

Low-level jets (LLJs) are narrow regions of relatively strong winds that occur within the MABL.

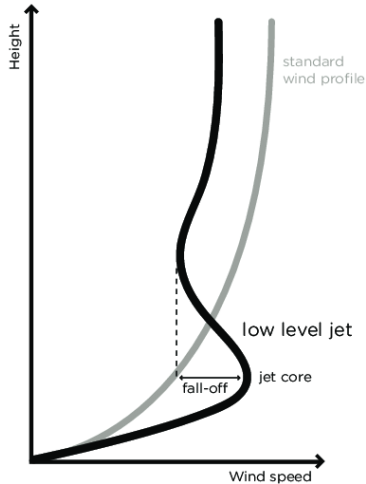


**Figure 1.** Depiction of both a low-level jet (black) and a typical (ideal) wind profile (gray)<sup>3</sup>.

Figure 1 illustrates both a logarithmic wind profile (gray) and wind profile containing an LLJ (black). The LLJ is characterized by a local maximum wind speed that is greater than the surrounding flow. This is distinctly visible in the profile. The maximum is labeled as the “jet-core”, also commonly referred to as the “nose” of the LLJ. Above this nose, wind speeds begin to decrease with height before gradually increasing again like an ideal wind profile would.

LLJs occurring in the Great Plains regions have been extensively studied, but LLJs also occur off the Eastern coast. These coastal LLJs are not as well explored and remain less understood<sup>4</sup>.

Characterizing LLJs and their stability regimes is important because they influence boundary layer structure. By improving the characterization of LLJs and stability regimes, this research supports NASA’s broader efforts in atmospheric dynamics and renewable energy applications. Wind Forecast Improvement Project 3

The third Wind Forecast Improvement Project (WFIP-3) is a multi-agency research campaign aimed at improving the understanding of physical

processes that govern wind variability and structure within the MABL, particularly in the context of offshore wind resource assessment<sup>5</sup>. WFIP-3 builds upon the previously successful campaigns, WFIP-1 (2011-2013) and WFIP-2 (2015-2019), which were both conducted over land. The transition to an offshore-focused campaign highlights the need to better understand wind behavior in marine environments since the observational data there is more limited than over land<sup>6</sup>.

The WFIP-3 campaign took place in the offshore New England region, with planning efforts beginning in September 2023, like completing permitting and land use agreements. The primary field campaign occurred throughout 2024, with the deployment of a barge for observation occurring twice. WFIP-3 concluded in October 2025.

WFIP-3 was a collaborative effort with several organizations involved including the National Oceanic and Atmospheric Administration (NOAA) and Department of Energy (DOE).

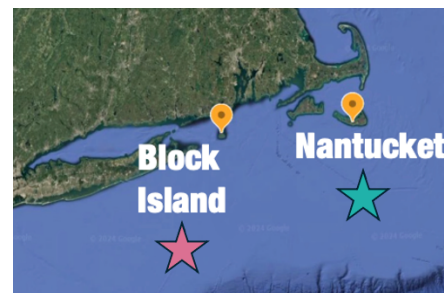


**Figure 2.** WFIP-3 sites: Block Island, RI (BLOC) & Nantucket, MA (NAN). Image provided by Timothy A. Myers (NOAA Physical Sciences Laboratory).

Figure 2 shows the two WFIP-3 sites used in this research: Block Island, RI (BLOC) and Nantucket, MA (NAN). These sites were selected because of their locations which experience differences in coastal exposure and marine influence.

## Data & Models

### High-Resolution Rapid Refresh

This study utilizes data from the High-Resolution Rapid Refresh (HRRR) model. The HRRR has a three-kilometer horizontal resolution and is updated hourly<sup>7</sup>. This work uses extracted column data at the BLOC and NAN WFIP-3 sites, with HRRR data evaluated only at those specific locations. Only 00 UTC-initialized forecasts are considered. Data is from January 2023 through December 2025.

Meteorological variables provided by the HRRR are extensive; this work specifically focuses on height (m), temperature at the LLJ nose height (°C), wind speed (ms<sup>-1</sup>), and wind direction (degrees).

The benefit of using HRRR data is high spatial and temporal resolution which is necessary to capture LLJ structures.

### Instruments

This analysis currently incorporates output from the HRRR model. Observational data obtained from the WFIP-3 campaign will be integrated in subsequent phases of this work.

Instruments deployed as a part of WFIP-3 that provide data include infrared spectrometers (ASSIST-II units, LR Tech), microwave radiometers (MP-3000 units, Radiometrics), and ceilometers for boundary layer structure assessment. Additional datasets include surface analysis maps, WFIP-3 model fields, and radar and weather maps for synoptic-scale pattern evaluation<sup>8</sup>.

Both model and observational data were analyzed using Python.

### LLJ Criteria

To systematically identify and classify LLJs, this study follows established criteria adapted from Whiteman et al. (1997)<sup>9</sup> and Vanderwende et al. (2015)<sup>10</sup>. The lowest wind speed maximum within the vertical wind profile is first identified. This maximum must exceed 10 ms<sup>-1</sup> and occur below 750 m. Additionally, wind shear above the jet nose

must exceed 3 ms<sup>-1</sup> to ensure a well-defined jet structure. Using a consistent set of criteria when isolating LLJ events is crucial to maintain objectivity and reproducibility.

### Line Integration Method

A line integral approach was introduced to estimate temperature changes over a finite region using data from three or more observation points<sup>11</sup>. This method is based on calculating temperature advection by relating the wind field to the horizontal gradient over a closed region.

The formula used can be derived from Green's Theorem (Equation 1), representing that a line integral around a closed curve equals a double integral over the enclosed area.

$$\oint_C P dx + Q dy = \iint \left( \frac{\partial Q}{\partial x} - \frac{\partial P}{\partial y} \right) dA \quad (1)$$

In Equation 1,  $C$  is the closed boundary around area  $A$ .  $P$  and  $Q$  are functions of space.

If the functions are defined using variables that represent wind components ( $u$ ,  $v$ ) and temperature ( $T$ ), Green's Theorem can be used to express the flux of temperature along the boundary using the processes occurring within the areas. After substituting and simplifying, Equation 2 is produced:

$$-\vec{V} \cdot \nabla T = - \left( u \frac{\partial T}{\partial x} + v \frac{\partial T}{\partial y} \right) \quad (2)$$

Where  $\vec{V}$  is the horizontal velocity vector and  $\nabla T$  is the horizontal temperature gradient. Equation 2 represents rate of temperature change due to horizontal transport by the wind<sup>11</sup>.

This methodology was successfully implemented to calculate temperature advection for select LLJ case dates using the BLOC and NAN sites, along with an additional offshore barge location. Initial investigation in this work has been limited to HRRR model data due to the incomplete

processing of WFIP-3 observational datasets, however, the HRRR-based implementation has been fully developed and applied to certain LLJ cases.

### Results

Southerly coastal LLJs being correlated with enhanced surface stability and warm air advection was previously hypothesized because, typically, warm tropical air travels with the winds from the south. This work successfully isolated several LLJ cases using the HRRR data and plotted them in Figures 3 and 4.

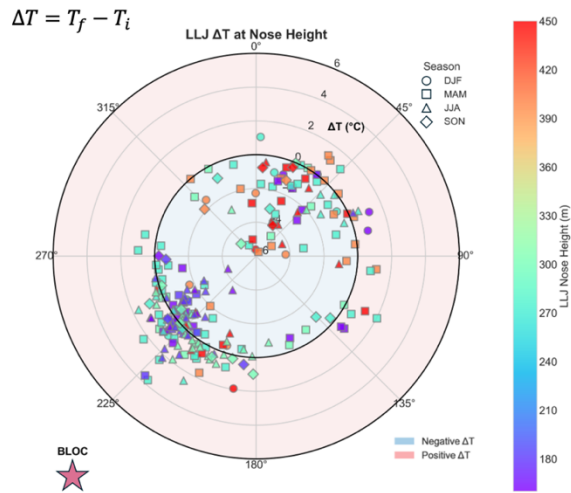


**Figure 3.** Radial plot depicts detected LLJ cases and their direction, local temperature change at LLJ nose height, nose height, and season at the BLOC site. Radial distance corresponds to  $\Delta T$  ( $^{\circ}\text{C}$ ), colors indicate LLJ nose height (m), and shapes represent seasons: DJF, MAM, JJA, SON.

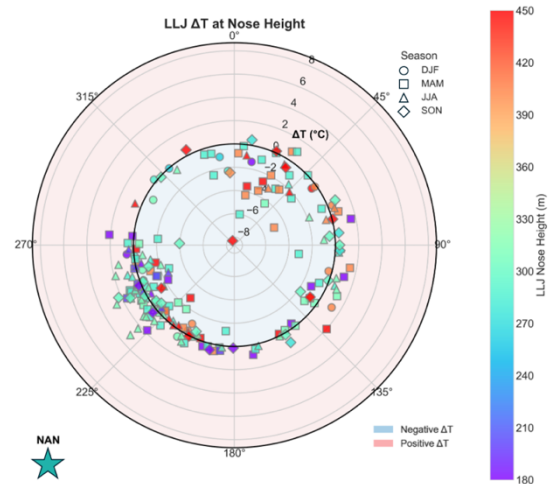


**Figure 4.** Radial plot depicts detected LLJ cases and their direction, local temperature change at LLJ nose height, nose height, and season at the NAN site. Radial distance corresponds to  $\Delta T$  ( $^{\circ}\text{C}$ ), colors indicate LLJ nose height (m), and shapes represent seasons: DJF, MAM, JJA, SON.

LLJ occurrences at both sites are concentrated primarily within the northeast and southwest directional sectors. Events at BLOC exhibit tighter clustering compared to NAN, suggesting stronger directional consistency. This could potentially be influenced by differing coastal geometry and land-sea interaction processes.

Despite the previous hypothesis, Figures 3 and 4 also suggest notable variability of the relationship between LLJ direction and  $\Delta T$ , suggestive of temperature advection. While southerly LLJs were expected to be correlated with a positive  $\Delta T$ , the results show that southerly LLJs exhibit both positive and negative  $\Delta T$  values. In contrast to this, northerly LLJs are predominantly associated with a negative  $\Delta T$ .

BLOC	<250m	250-350m	>350m
N	10	37	34
	Total N Cases		81
S	58	78	18
	Total S Cases		154
Freq of all N	0.12	0.46	0.42
Freq of all S	0.38	0.51	0.12

**Table 1.** Detected LLJ case counts/frequencies by origin direction (North or South) and nose height (<250m, 250-350m, >350m) for BLOC site.

NAN	<250m	250-350m	>350m
N	6	31	26
	Total N Cases		63
S	25	85	25
	Total S Cases		135
Freq of all N	0.1	0.49	0.41
Freq of all S	0.19	0.63	0.19

**Table 2.** Detected LLJ case counts/frequencies by origin direction (North or South) and nose height (<250m, 250-350m, >350m) for NAN site.

Differences in LLJ vertical structure are also evident in the results. Tables 1 and 2 show that at both sites northerly LLJs occur more frequently at higher altitudes (greater than 350 m in height), whereas southerly LLJs are more commonly observed at lower altitudes (less than 250 m in height). These patterns indicate systematic differences in jet structure that may reflect forcing mechanisms or other environmental influences.

A tendency for lower-altitude southerly jets may be associated with more stable near-surface conditions, as previously hypothesized, while higher-altitude northerly jets may be due to stronger shear or similar synoptic factors.

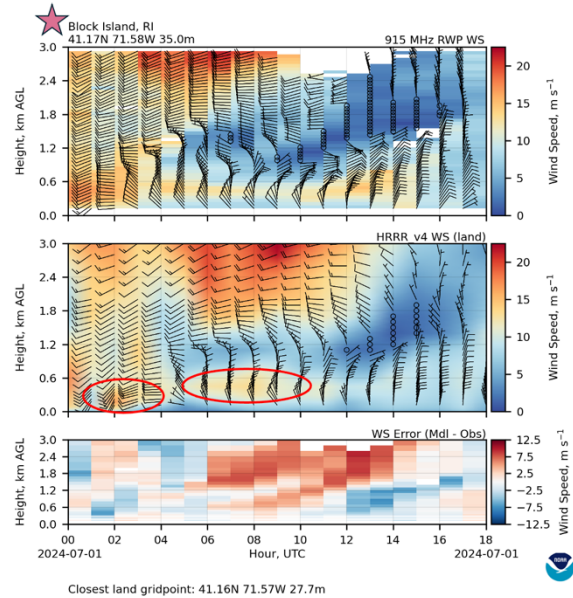


**Figure 5.** 915 MHz Radar Wind Profiler 00 UTC at BLOC for July 1, 2024<sup>12</sup>.

A representative LLJ case at BLOC from July 1, 2024 (Figure 5) illustrates these nose height relationships. Circled in the second panel (HRRR model) of Figure 5 are two different LLJ events. The leftmost case, exhibiting southwesterly flow, appears to occur at a lower altitude than the case on the right, which exhibits predominantly northerly flow. Although one case of many, Figure 5 shows consistency among the statistical patterns identified across the dataset. Furthermore, these cases highlight the complexity and variability possible in different LLJ events.

### Conclusion

Overall, this study yielded results that enhance the understanding of coastal LLJ characteristics and associated local temperature changes within the MABL. It was found that LLJs are not always driven by the expected warm southerly flow. This means that flow direction alone does not uniquely determine the thermodynamic evolution at the jet nose height suggesting that other processes such as vertical mixing,

air-sea interactions like the sea-land breeze cycles, and divergence stemming from passing frontal boundaries may play a significant role in modulating temperature changes.

The observed differences in LLJ vertical structure compared to direction further support the presence of distinct dynamics occurring within the MABL. The results suggest the influence of both local stability conditions coupled with large-scale forcings rather than a single mechanism.

Beyond this present analysis, a foundation for continued investigation of temperature variability associated with LLJs was established. The previously developed line integral framework provides a pathway to further explore temperature advection using HRRR output. The implementation of this code and consideration of newly usable WFIP-3 observational data presents an opportunity to grow this research.

These findings underscore the importance of coastal LLJs as underexplored components of the MABL. Their variability in structure, height, and temperature changes have direct implications for offshore wind energy production, boundary layer forecasting, and air-sea interaction processes. Improved characterization of these jets is critical to advance scientific understanding. This work contributes to broader efforts aligned with NASA's atmospheric science and renewable energy initiatives, while also supporting Virginia's offshore wind development goals, reinforcing the state's leadership in clean energy innovation.

### **Future Work**

This work's observations of directional clustering and nose-height dependence motivate a further investigation of LLJ duration, diurnal cycles, and forcing mechanisms. Potential future work will focus on further characterizing LLJ temporal behavior, including duration and diurnal

variability, to better understand the processes influencing temperature changes at the jet nose height.

Expanding the analysis to incorporate fully processed WFIP-3 observational data will allow validation of HRRR-based results and provide a better picture of LLJ dynamics. Continued application of the line integral framework will enable an investigation of temperature gradients and other influences such as coastal circulations and surface stability.

Future work will further improve understanding of LLJ structure, evolution, and thermodynamic impacts, ultimately strengthening predictive modeling in atmospheric science.

### **Acknowledgements**

The author would like to thank the Virginia Space Grant Consortium (VSGC) for their financial support of this research and the opportunity to participate in this work. The author also acknowledges support from Hampton University and the faculty and mentors who provided guidance through this project.

### **References**

- [1] Fairall, C. W. (1992). *Boundary Layer Processes in Coastal Meteorology: Prospects for Remote Sensing Applications*. Wave Propagation Laboratory, Boulder, CO.
- [2] Wagner, C., Smith, T., & Liu, C. (2020). *Advances in Wind Energy Forecasting and Turbulence Mitigation Using Remote Sensing and NASA Technologies*. NASA Technical Report.
- [3] Hallgren, C., Arnqvist, J., Ivanell, S., Körnich, H., Vakkari, V., & Sahlée, E. (2020). Looking for an Offshore Low-Level Jet Champion among Recent Reanalyses: A

Tight Race over the Baltic Sea. *Energies*, 13(13), 3670.

[4] De Jong, E., Quon, E., & Yellapantula, S. (2024). Mechanisms of Low-Level Jet Formation in the U.S. Mid-Atlantic Offshore. California Institute of Technology and National Renewable Energy Laboratory.

[5] Djalalova, I., Bianco, L., Wilczak, J. M., et al. (2021). *Marine boundary layer characteristics and implications for offshore wind energy forecasting*. *Journal of Atmospheric and Oceanic Technology*, 38(5), 895-913.

[6] Pacific Northwest National Laboratory (PNNL). (2025). Wind Forecast Improvement Project 3: Overview. *PNNL*. <https://www.pnnl.gov/projects/wind-forecast-improvement-project-3/>

[7] NOAA Rapid Refresh (HRRR). NOAA/NWS. <https://rapidrefresh.noaa.gov/hrrr/>

[8] Pacific Northwest National Laboratory (PNNL). (2025). Wind Forecast Improvement Project 3: Instruments. *PNNL*. <https://www.pnnl.gov/projects/wind-forecast-improvement-project-3/instruments>

[9] Whiteman, C. D., Zhong, S., & Bian, X. (1997). The influence of the diurnal cycle of the boundary layer on low-level jet development over complex terrain. *Journal of Applied Meteorology*, 36(9), 1133-1149.

[10] Vanderwende, B. C., Doran, J. C., & Cline, J. D. (2015). Low-level jet formation and its role in the transport of moisture and heat in the central United States. *Journal of Climate*, 28(9), 3475-3495.

[11] Wagner, T. J., Turner, D. D., Heus, T., & Blumberg, W. G. (2022). Observing profiles

of derived kinematic field quantities using a network of profiling sites. *Journal of Atmospheric and Oceanic Technology*, 39(3), 335–351.

[12] NOAA Physical Sciences Laboratory (2025). *WFIP3 Model and Observations Portal*. [https://psl.noaa.gov/renewable\\_energy/wfip3/modelobs/](https://psl.noaa.gov/renewable_energy/wfip3/modelobs/)